(Received 20 October 2023, Accepted 29 November 2023, Scheduled 8 December 2023)

Performance Enhancement of High-gain STDA Antennas with Reflector for 4G LTE and Sub-6 GHz 5G Applications: Design, Measurement, and Analysis

Mohd Wasim[1], Shelej Khera[1], Tanvir Islam[2], Praveen Kumar Malik[1], Sivaji Asha[3], and Sudipta Das[4*]

[1]*School of Electronics and Electrical Engineering, Lovely Professional University, Phagwara 144411, India*
[2]*Department of Electrical and Computer Engineering, University of Houston, Houston, TX 77204, USA*
[3]*Saveetha Engineering College, Saveetha Nagar, Thandalam, Chennai-602105, India*
[4]*Department of Electronics and Communication Engineering, IMPS College of Engineering and Technology, Malda-732103, West Bengal, India*

ABSTRACT: The paper focuses on the design, measurement, and performance analysis of a high-gain cross-orthogonal series fed two dipole antenna (STDA) arrays with side-wall reflectors. The antenna is specifically designed for 4G Long Term Evolution (LTE) and sub-6 GHz 5G band applications. The designed antenna is capable of operating at multiple frequencies aiming to support 4G LTE and the sub-6 GHz 5G application bands. To improve the radiation characteristics and prevent coupling effects in the presence of side-wall reflectors, parasitic strip pair directors are included in the antenna design. Furthermore, the performance of the designed STDA is evaluated by forming different array configurations, such as 2×1, 2×2, and 2×3 arrays. The various array configurations are proposed to investigate the effect of the projected array arrangements on the radiation pattern, impedance bandwidth, and gain characteristics. The results of the measurements show that the radiation characteristics of the antenna have been improved significantly. The proposed antenna operates at six distinct frequencies for $S_{11} \leq 10$ dB. The operating frequencies at 1.8, 2.35, and 2.6 GHz can be utilized for LTE and 3.2, 4.2, and 5.2 GHz which can support sub-6 GHz 5G bands. The antenna is characterized by its compact size, measuring around 89 mm $\times$ 71 mm, while still achieving high gain of 12.3 dB for single STDA element with parasites and with reflector. These results emphasize the importance of the proposed design, which incorporates parasitic strip pair directors and side-wall reflectors. This design methodology plays a crucial role in enhancing the performance of the prescribed STDA array for both 4G LTE and sub-6 GHz 5G applications.

1. INTRODUCTION

The advent of 5G technology has led to the development of new 5G frequency bands, including sub-6 GHz bands. These bands are well-suited for wide coverage and enhanced penetration through obstacles, making them ideal for applications such as rural broadband and fixed wireless access [1–3]. Different countries have adopted their own frequency band plans for 5G services, but the majority have allocated the sub-6 GHz bands. This is because these bands offer a good balance of range and capacity, making them suitable for a wide range of use cases [4–6]. The introduction of these new frequency bands holds promise for faster and more reliable communication in the near future. Multiple-input multiple-output (MIMO) systems can also play a critical role in 5G networks, as they can improve channel capacity and communication reliability. However, meeting the stringent requirements of 5G technology may necessitate the use of larger MIMO antenna arrays [7–9]. Antennas are designed for good performance in terms of efficiency, peak gain, and radiation patterns supporting multiple wireless standards [10]. Integrating existing MIMO 4G wireless standards with emerging 5G standards is challenging due to space and gain requirements. Despite these challenges, MIMO technology significantly enhances data transmission rates, coverage, and reliability. As the industry innovates and overcomes obstacles, significant advancements in 5G networks are anticipated [11–14]. Series-fed two dipole array antennas are well suited for 4G and 5G communication bands due to their wide bandwidth and ease of miniaturization. The configuration consists of two dipole antennas connected in series, achieving higher gain than a single dipole antenna. By forming a massive array with a large number of these antennas, high-gain can be achieved. The number of antennas can be adjusted to achieve the desired gain and bandwidth [15–17]. Series fed two dipole antenna arrays are reported in [18, 19] using parasitic elements which exhibit an operating bandwidth of 1.7 to 2.7 GHz, covering various LTE bands. Parasitic elements are a type of antenna element that improves gain and directivity by radiating electromagnetic waves. They are shorter than dipole elements and not excited by the feed, but are affected by the electromagnetic field from the dipole elements. This radiation adds to the dipole radiation, reducing sidelobe levels. By introducing parasite elements, antenna radiation patterns can be shaped to achieve better performance in terms of gain, directivity, and sidelobe levels. This is useful in wireless commu-

* Corresponding authors: Sudipta Das (sudipta.das1985@gmail.com).

nication systems where high gain and directivity are important for longer range and better signal quality. The series-fed two dipole array antenna with Yagi-Uda configuration has gained significant recognition as a versatile antenna well-suited for applications requiring high gain and directivities, such as radar and satellite communication [20–22]. Furthermore, a method to minimize mutual coupling in MIMO antennas is presented using a parasitic fragment-type element. This element utilized a multi-objective optimization search to divide the space between the antennas into cells and selectively metalize certain cells to achieve desired isolation and return losses [23, 24]. Reflectors can increase or decrease mutual coupling among multiple antennas depending on their placement and size. Reflectors close to antennas increase mutual coupling, while those far away decrease it. The parasitic fragment-type element placed between two antennas reduces the mutual coupling by reflecting electromagnetic waves from one antenna back to the other, achieving a maximum isolation of 29 dB. This technique did not significantly impact radiation patterns, making it a promising and easy-to-implement method for suppressing mutual coupling [25]. The use of parasitic fragment-type elements also offers greater flexibility and versatility than conventional isolation techniques, resulting in substantial improvements in isolation, diversity performance, radiation patterns, and radiation efficiency of antenna structures reported in [26, 27]. Single radiator antennas are simple and cost-effective but have lower gain than array antennas, making them less suitable for long-distance communication. The large antenna array usually offers higher gain and a more directional radiation pattern, making it more suitable for long-distance communication. Researchers used CST Microwave Studio software to optimize the performance of the 64-element array antenna, ensuring that it met the requirements of 5G and other communication systems but at the cost of more complex and expensive structure [28].

These motivate the authors of this article to design a low cost and less complex antenna array structure to provide useful performance in terms of operating bands, mutual coupling reduction, gain and directional patterns. In order to achieve the design goals, Series Fed Two Dipole Antenna (STDA) array in 2×1, 2×2, and 2×3 configurations with sidewall reflectors are designed and discussed in this article.

In this article, a proposed method is presented to improve the performance of the STDA by increasing its bandwidth and reducing coupling losses. The methodology encompasses the integration of a parasitic strip pair director into the established STDA array configuration, strategically positioned adjacent to the upper dipole element, alongside the introduction of sidewall reflectors. In this STDA analysis, each element is enabled with a parasitic element, which is analyzed using a sidewall reflector to achieve better performance. The investigation conducted by the authors delves into the intricate relationship between the precise placement and dimensions of the parasitic strip pair director and its consequential impact on the antenna's overall performance. Through their investigation, the authors find that the introduced parasitic strip pair director plays a crucial role in enhancing the conventional STDA array's performance by expanding bandwidth, increasing gain, and mitigating coupling losses. The proposed research employs a systematic approach to analyze STDA arrays with reflectors in various configurations. The coupling losses are measured by considering different array arrangements and reflector positions. The performance of each configuration is assessed in terms of radiation pattern, gain, and coupling reduction. The design and parametric optimization of the proposed antenna is conducted using CST Microwave Studio 2018 software, a powerful tool for simulating and optimizing antenna designs. The software facilitated the optimal performance of three different array configurations, allowing to achieve desired performance characteristics with a comprehensive performance evaluation. The findings highlight the potential of this technique to improve the overall performance of traditional STDA arrays for various communication applications such as 4G LTE and Sub-6 GHz 5G.

2. DESIGN METHODOLOGY

2.1. Design of STDA Array with Parasitic Director and Reflectors with Side Walls

Figure 1 illustrates the STDA array design that incorporates a parasitic director. Parasitic directors in STDA arrays play a crucial role in enhancing antenna performance. The parasitic directors focus the radiation pattern in the forward direction, increasing directivity. The antenna is composed of two unequal strip dipole components, namely dipole 1 (D_1) and dipole 2 (D_2), which are discernible by their respective lengths, L_1 and L_2, and widths, W_1 and W_2. The length of the long dipole controls the lower operating frequency, while the length of the short dipole controls the upper operating frequency. The grounding structure (R_0) is characterized by dimensions L_{gp} and W_{gp} in length and width, respectively. The separation distance between R_0 and D_1 is denoted as S_1, while the distance between D_1 and D_2 is denoted as S_2. The proposed antenna configuration entails the addition of a parasitic strip pair director (D_{pr}) to the conventional STDA array, which are strategically positioned D_{pr} units away from D_2. An integrated balun is used to match the input impedance of the antenna to the 50 Ω feed line. It consists of a microstrip line and a coplanar strip line, with the end of the microstrip line shorted using a shorting pin at the feeding point.

Each strip in the parasitic pair is characterized by length l_d and width w_d, with a gap between them denoted as g_d. The parasitic director is a pair of parallel strips that are located a short distance behind D_2. The strips are fed in parallel with a 90-degree phase shift between them. This phase shift causes the currents on the strips to be in the opposite direction, which creates a stronger radiation pattern in the forward direction. The length and width of the parasitic director are chosen to optimize the gain and bandwidth of the antenna. The length of the strips is typically a few percent of the wavelength, and the width of the strips is typically a few times the skin depth. The gap between the strips is chosen to minimize the mutual coupling between them. The distance, often several times the skin depth, is commonly referred to as the gap. Within the context of the parasitic strip pair director, the design parameters that exert influence on antenna performance include the length, width, and spacing between the strips. The length governs the resonant frequency;

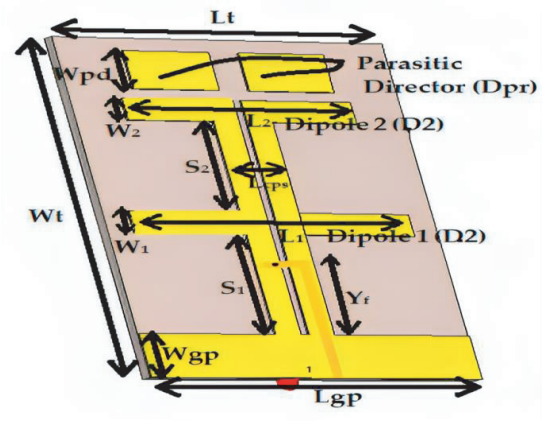

FIGURE 1. STDA with parasites elements.

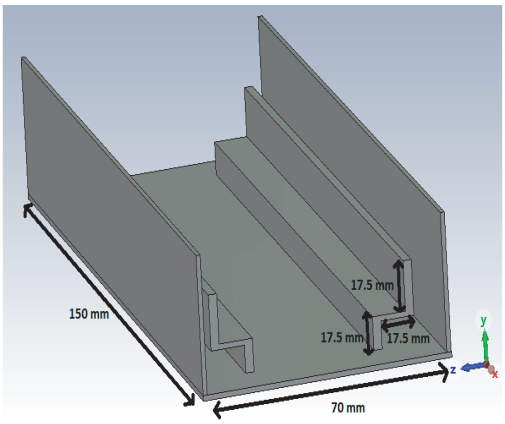

FIGURE 2. Reflector with sidewalls.

FIGURE 3. Fabricated view with measurement result.

the width controls the bandwidth; and the gap regulates the mutual coupling between the strips. To achieve maximum bandwidth and stable gain in the band, the length should be a few percent of the operating wavelength, the width should be a few times the skin depth, and the gap should be a few times the skin dept. Design parameters of a parasitic director of a strip pair (length, width, and gap) have been analyzed to achieve maximum bandwidth and a stable gain in the band. Director strip has been analyzed including three parameters: length of the strips, width of the strips, and gap between the strips. The return loss and gain characteristics are observed for various values of these parameters. The spatial separation, typically several times the skin depth, is conventionally denoted as the gap. In the realm of the parasitic strip pair director, the design parameters that intricately impact the antenna's performance encompass the length, width, and inter-strip spacing. The length governs the resonant frequency; the width governs the bandwidth; and the gap governs the mutual coupling between the strips. The values (in mm) that are deemed optimal for ensuring impedance matching and consistent gain across a broad frequency band are represented as: $L_1 = 56.8$, $L_2 = 32.8$, $L_{gp} = 71$, $S_1 = S_2 = 23.5$, $W_1 = W_2 = 9.8$, $L_{cps} = 20$, $W_{gp} = 10$, $L_t = 71$, $W_t = 89$, $h = 1.6$, $y_f = 15.3$, and $W_{pd} = 11.6$. A reflector with ladder sidewalls has been designed, featuring dimensions of 150 mm $\times$ 70 mm. The sidewalls are designed with folds measuring 17.5 mm, which is presented in Figure 2. These side walls help in shaping and directing the waves even further. They prevent signal leakage to the sides and back of the antenna, ensuring that most of the energy is directed toward the desired target. By strategically arranging and controlling the individual antennas in the array, this system can achieve exceptional performance in terms of gain, directivity, and versatility, making it valuable for a wide range of applications in the field of wireless communication.

The fabricated STDA array with parasitic elements has been designed and tested using Agilent N9923A FieldFox RF Vector Network Analyzer. The fabricated prototype along with measured result is presented in Figure 3.

2.2 STDA with Reflectors in Different Configurations

This research contributes to the understanding of coupling losses in STDA arrays with reflectors. The study demonstrates the effectiveness of different configurations in reducing coupling effects and improving overall antenna performance. The findings serve as a valuable reference for future design and optimization of STDA arrays for wireless communication applications. The concept of measuring the coupling loss between

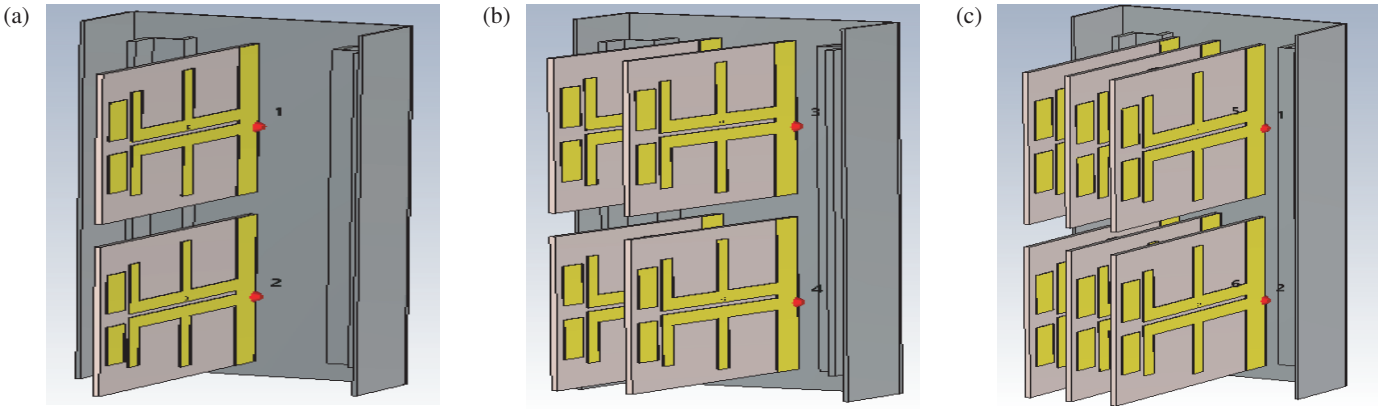

FIGURE 4. STDA with reflector in different arrays configuration. (a) 2×1. (b) 2×2. (c) 2×3.

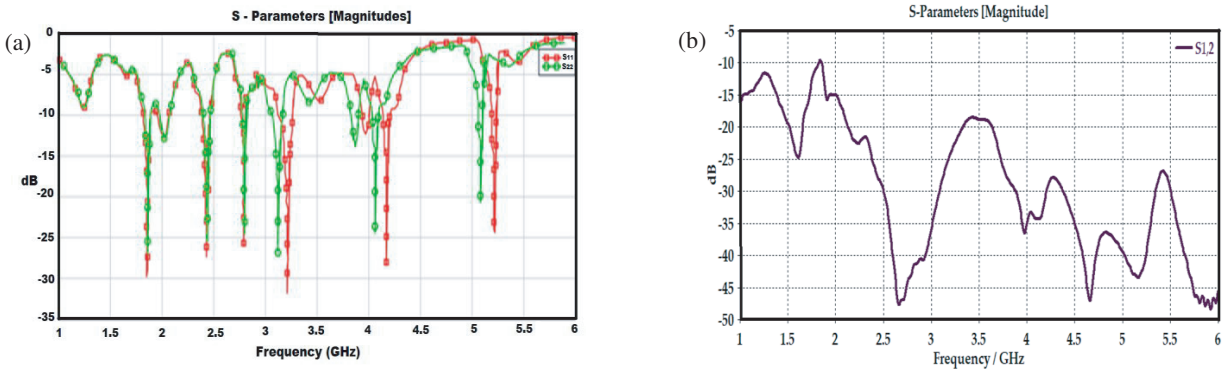

FIGURE 5. STDA 2×1 array configuration. (a) Reflection Coefficients (S_{11} and S_{22}). (b) Mutual Coupling (S_{12}).

the array elements relates to understanding how the individual antennas in the array interact with each other. The relative distances between the elements influence the phase relationship and, consequently, the combined radiation pattern of the array. The proposed design aspect focuses on utilizing different array configurations to measure the coupling loss between the array elements, providing insights into the interaction and performance of the antennas within the array system. Parasitic arrays are widely used in antenna designs to shape radiation patterns and enhance performance. The spacing between antenna elements plays a crucial role in achieving desired radiation characteristics while minimizing coupling interference. The research adopts a systematic approach to design and analyze a parasitic array with improved element spacing. The proposed design is based on the finding that a properly designed parasitic array with a spacing of 0.1λ to 0.15λ can provide desirable frequency bandwidth, gain, and front-to-back ratio.

The research employs a systematic approach to analyze reflection coefficients and measure coupling losses in different STDA array configurations. The 2×1, 2×2, and 2×3 array configurations have been designed shown in Figures 4(a), (b), and (c) and are considered to evaluate the performance. The array configurations are designed to analyze the coupling losses with reflectors. The array configurations are studied to understand how different arrangements of arrays and reflectors affect the amount of energy lost during coupling and the overall amplification of the signal.

Coupling losses are found to quantify the interaction between the array elements. Reflection coefficients are calculated to assess the impedance matching and power reflection characteristics of the antennas in each configuration. Array with reflector in different configurations has been simulated and discussed.

2.3 Reflection Coefficients and Mutual Coupling with Reflectors

The simulated results demonstrate the effectiveness of reflectors in reducing coupling effects between array elements. The impact of reflector positions and array arrangements on mutual coupling losses is quantified, providing important information for optimizing the antenna design. The research investigates different configurations of STDA arrays, including 2×1, 2×2, and 2×3 setups. The focus lies on finding return loss and evaluating coupling between array elements using S-parameters. In each configuration, reflection coefficients are assessed at various ports to understand power reflection, while coupling between specific ports is measured to quantify interactions between elements.

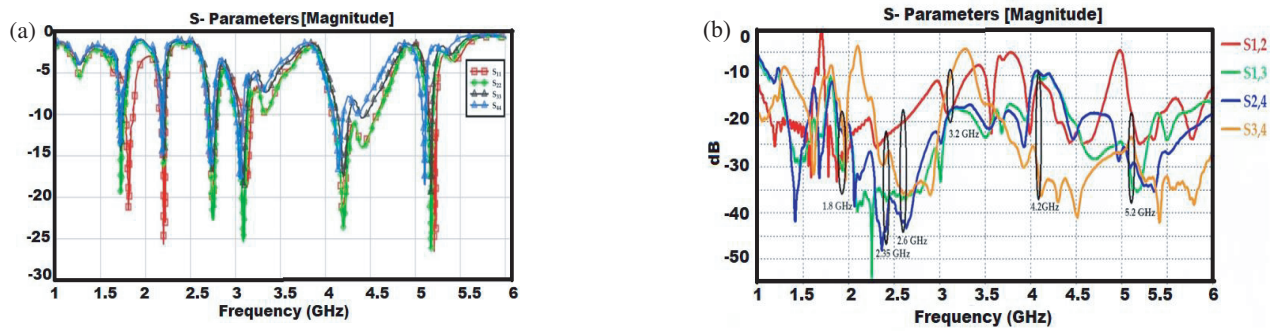

FIGURE 6. STDA 2×2 array configuration. (a) Reflection Coefficients (S_{11}, S_{22}, S_{33}, S_{44}). (b) Mutual Coupling (S_{12}, S_{13}, S_{24}, S_{34}).

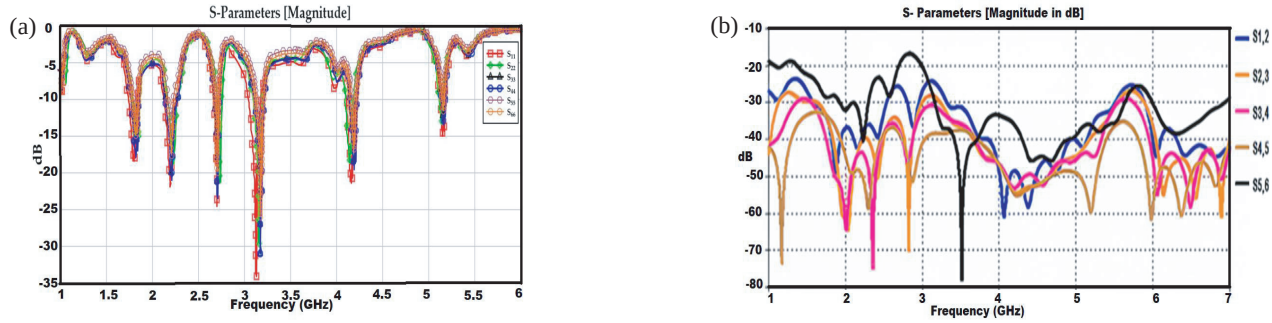

FIGURE 7. STDA 2×3 array configuration (a) Reflection Coefficients. (S_{11}, S_{22}, S_{33}, S_{44}, S_{55}, S_{66}). (b) Mutual Coupling (S_{12}, S_{13}, S_{24}, S_{34}, S_{45}, S_{56}).

Frequency (GHz)	Gain (dB)	
	Simulation	Measurement
1.8	8	7.4
2.35	12	11.1
2.6	11.4	12.3
3.2	10.8	10.3
4.2	5	5.9
5.2	7.3	6.1

TABLE 1. Measured and simulated gain comparison.

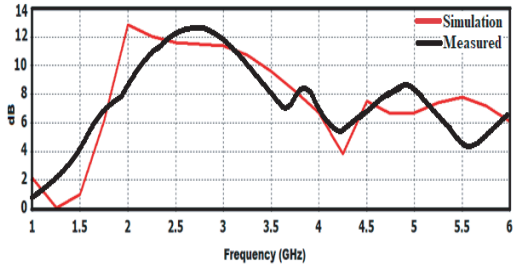

FIGURE 8. Measured and simulated Gain of Single element STDA.

2.3.1. STDA 2×1 Array Configuration

The array 2×1 STDA has two dipole antennas and two ports, and S_{11} and S_{22} are simulated for the return loss measurement, and S_{12} and S_{21} hav been accounted for the measuring of the coupling loss. The spacing between the two elements is 36.5 mm, and it is obtained after multiple iterations of coupling loss reduction. In Figures 5(a) and (b), S-parameters like S_{11} and S_{22} represent the input port voltage reflection with coefficient, while S_{22} represents the output port voltage reflection with coefficient. On the other hand, S_{12} represents the forward voltage gain, while S_{21} represents the reverse voltage gain, which is used to measure the coupling loss. The designed array operates at multiple resonant frequencies to be utilized for 4G LTE and Sub-6 GHz 5G with significant amount of return loss and mutual coupling as depicted in Figures 5(a)–(b).

2.3.2. STDA 2×2 Array Configuration

The research employs a systematic approach to simulated return loss and evaluate coupling in the 2×2 STDA array. Figures 6(a) and 6(b) show the return loss and coupling loss effect. Return loss is calculated at ports S_{11}, S_{22}, S_{33}, and S_{44} to assess the antenna's ability to reflect incident power. Coupling among ports S_{12}, S_{13}, S_{24}, and S_{34} is simulated to quantify the level of interaction between the array elements. The simulations are performed using appropriate test setups and equipment.

2.3.3. STDA 2×3 Array Configuration

The research employs a systematic approach to simulated return loss and evaluates coupling in the 2×3 STDA array. Figures 7(a) and 7(b) present the reflection coefficients and mutual coupling parameters. Reflection coefficients are calculated at ports S_{11}, S_{22}, S_{33}, S_{44}, S_{55}, and S_{66} to assess the antenna's

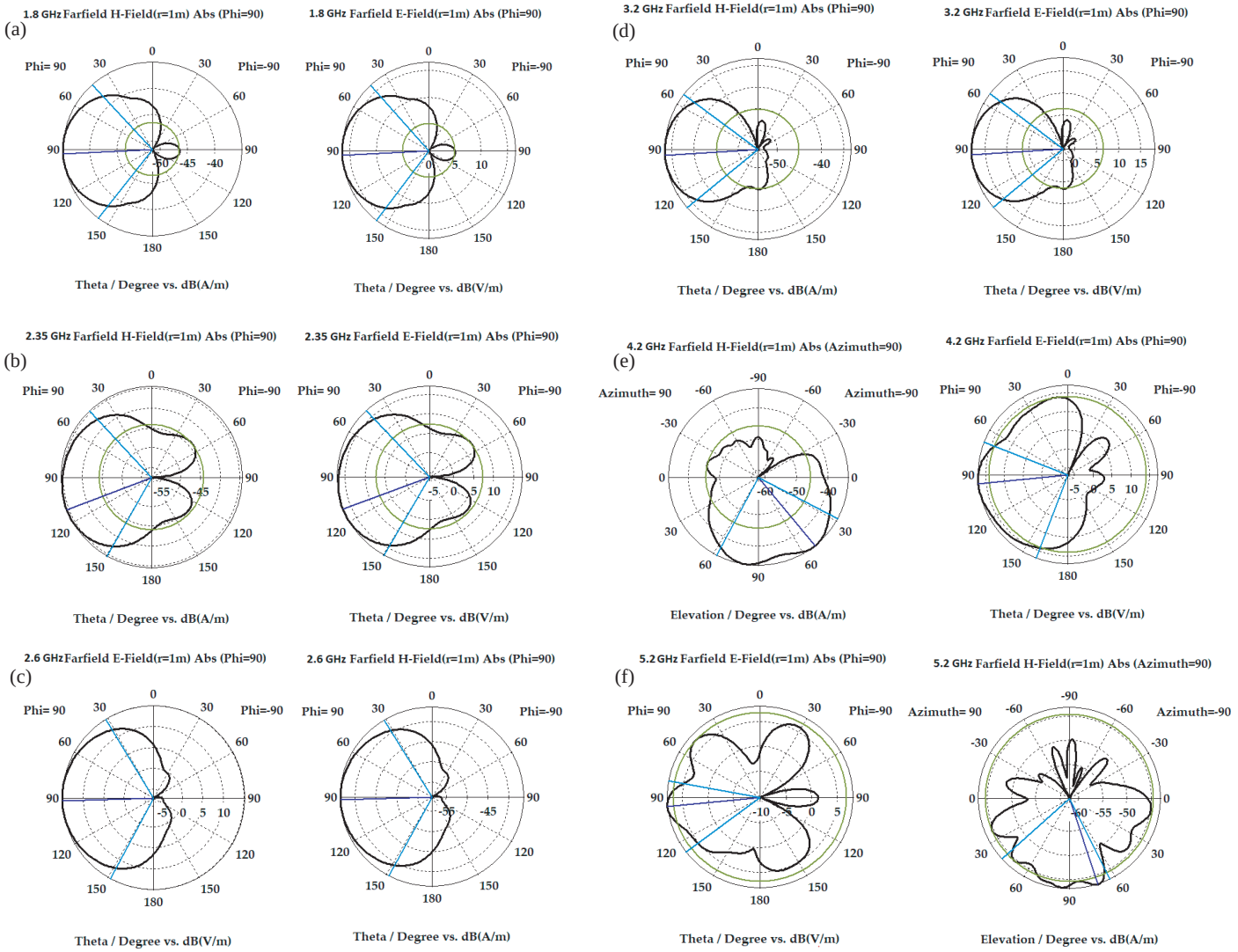

FIGURE 9. Measured E and H plane radiation patterns of element 1 at (a) 1.8 GHz, (b) 2.35 GHz, (c) 2.6 GHz, (d) 3.2 GHz, (e) 4.2 GHz, (f) 5.2 GHz.

ability to reflect incident power. The coupling among ports S_{12}, S_{23}, S_{34}, S_{45}, and S_{56} is simulated to quantify the level of interaction between the array elements. The simulations are performed using appropriate test setups and equipment. Figures 7(a) and (b) show the optimum effects of mutual coupling and return loss at 4G LTE and Sub-6 GHz 5G bands. The suggested STDA 2×3 array functions at multiple resonant frequencies of which, 1.8, 2.35, and 2.6 GHz can be utilized for 4G LTE, and 3.2, 4.2, and 5.2 GHz can be used for sub-6 GHz 5G communication applications. Furthermore, the designed array 2×3 maintains minimum mutual coupling of -24.9 dB. The mutual coupling varies from -24.9 dB to 44 dB across the operating bands.

Analyses shown in Figures 5, 6, and 7 present reflection coefficients and mutual coupling of different configurations of two, four, and six aligned antennas with sidewall reflectors across a frequency range of 1.8 to 5.2 GHz. Reflection coefficients are measured to account for the loss of power that signal reflected back from an antenna, rather than being transmitted. Mutual coupling, on the other hand, refers to the interaction between two or more antennas that are close together. As strong mutual coupling between the antennas has an impact on reflection coefficient, the use of reflectors and the iterative distance between the elements is kept stable and under control. Signals redirected to another antenna are effectively redirected back, indicating efficient transmission of signals and minimal power loss. The interaction among the antennas also cause a shift in resonant frequencies and changes in bandwidth, which are identified in the experiment. To stabilize the resonant frequencies and changes in bandwidth, the reflectors play a significant role in effectively transmitting or receiving signals. Finally, we studied the reflector effect of these antennas. The reflector surface reflects electromagnetic waves, and it helps to improve the performance of an antenna by directing the waves in a specific direction.

TABLE 2. Comparison of proposed antenna with several other antennas by examining their various characteristics.

Reference	Frequency bands/ Operating Frequencies (GHz)	Isolation	Average Gain (dB)	Size (mm^3)	XPD (Cross-polarization discrimination)
[29]	3.4–3.8	23	9	Not Given	25
[30]	3.3–3.6	28.8	8.2	$72 \times 72 \times 18.8$	24
[31]	3.65–3.81	31	10	$86 \times 81 \times 3$	23
[32]	3.3–3.6	25	7.3	$72 \times 72 \times 18.8$	24.5
[33]	3.28–3.7 & 4.75–5.0	40	8 & 10	$50 \times 50 \times 7.4$	20
Proposed	(1.8, 2.35, and 2.6) & (3.2, 4.2, and 5.2)	(24.9 to 44)	8–12.3	$89 \times 71 \times 1.6$	> 11.5

2.4. Radiation Patterns and Gain Characteristics

The simulated and measured gain variations with respect to various resonant frequencies are shown in Figure 8. The gain of the proposed antenna system at different frequencies is tabulated in Table 1. The measured gain in the range of 5.9 to 12.3 dB is achieved in the frequency band range of 1.8 to 5.2 GHz frequencies, respectively. The far-field radiation patterns for element 1 at different resonant frequency bands are measured and shown in Figures 9(a)–(f) for six functional frequencies, 1.8 GHz, 2.35 GHz, 2.6 GHz, 3.2 GHz, 4.2 GHz, and 5.2 GHz. The patterns are depicted for both E and H planes, representing polarization components phi and theta. It is important to note that the antenna exhibits similar radiation characteristics but with a perpendicular polarization shift. This shift in polarization ensures polarization diversity, which means that there is minimal correlation in the radiation patterns between individual elements in this antenna design.

3. PERFORMANCE COMPARISON OF PROPOSED STDA WITH OTHER DESIGNS

A comparative study has been conducted between the proposed antenna and previous designs [29–33]. The analysis has been executed by considering the operating frequency band, isolation, gain, antenna size, and XPD (Cross-polarization discrimination) parameters. The comparative results are summarized in Table 2. The results indicate that the proposed antenna can be fabricated with ease and offers dual-band performance despite its relatively small size. Additionally, this antenna boasts a good cross-polarization, as well as acceptable gains and isolation.

4. CONCLUSION

The article concludes with significant achievements in the design, measurement, and analysis of the high-gain cross-orthogonal Series-Fed Two Dipole Antenna (STDA) with side-wall reflectors, specifically tailored for 4G LTE and sub-6 GHz 5G applications. The STDA with compact dimensions of 89 mm $\times$ 71 mm demonstrates the capability to operate at multiple resonant frequencies, supporting both 4G LTE and sub-6 GHz 5G bands. The inclusion of parasitic strip pair directors and side-wall reflectors plays a pivotal role in enhancing the antenna's performance. The 2×1, 2×2, and 2×3 array configurations are systematically explored to understand their impact on radiation patterns, impedance bandwidth, and gain characteristics. The compact size of the antenna, coupled with high gain (13.7 dB), highlights its practical suitability and efficiency in real-world applications. The examination of mutual coupling and return loss in various array configurations (2×1, 2×2, and 2×3) provides valuable insights into the antenna's behavior. The mutual coupling is maintained at a minimum of -24.9 dB, ensuring efficient transmission of signals with minimal power loss. The reflector's role in stabilizing resonant frequencies and minimizing bandwidth changes is emphasized, contributing to the effective transmission or reception of signals. The far-field radiation patterns illustrate the antenna's consistent performance across different resonant frequencies, showcasing polarization diversity and low correlation between individual elements. A comparative study with previous designs underscores the proposed antenna's fabrication ease, multiband performance, good cross-polarization, acceptable gain and isolation. The operating frequencies at 1.8, 2.35, and 2.6 GHz can be utilized for LTE, and 3.2, 4.2, and 5.2 GHz can support sub-6 GHz 5G bands.

REFERENCES

[1] Ikram, M., R. Hussain, and M. S. Sharawi, "4G/5G antenna system with dual function planar connected array," *IET Microwaves Antennas & Propagation*, Vol. 11, No. 12, 1760–1764, Sep. 2017.

[2] Naqvi, S. I., A. H. Naqvi, F. Arshad, M. A. Riaz, M. A. Azam, M. S. Khan, Y. Amin, J. Loo, and H. Tenhunen, "An integrated antenna system for 4G and millimeter-wave 5G future handheld devices," *IEEE Access*, Vol. 7, 116 555–116 566, 2019.

[3] Ikram, M., N. Nguyen-Trong, and A. Abbosh, "Hybrid antenna using open-ended slot for integrated 4G/5G mobile application," *IEEE Antennas and Wireless Propagation Letters*, Vol. 19, No. 4, 710–714, Apr. 2020.

[4] Yang, M., Y. Sun, and F. Li, "A compact wideband printed antenna for 4G/5G/WLAN wireless applications," *International Journal of Antennas and Propagation*, Vol. 2019, 1–9, Sep. 2019.

[5] Nadeem, I. and D.-Y. Choi, "Study on mutual coupling reduction technique for MIMO antenna," *IEEE Access*, Vol. 7, 563–586, 2019.

[6] Al Abbas, E., M. Ikram, A. T. Mobashsher, and A. Abbosh, "MIMO antenna system for multi-band millimeter-wave 5G and wideband 4G mobile communications," *IEEE Access*, Vol. 7, 181 916–181 923, 2019.

[7] Ismail, N. B., M. T. Ali, N. N. S. N. Dzulkefli, R. Abdullah, and S. Omar, "Design and analysis of microstrip Yagi antenna for Wi-Fi application," in *2012 IEEE Asia-pacific Conference on Applied Electromagnetics (APACE)*, 283–286, Melaka, Malaysia, Dec. 2012.

[8] Chen, Y.-L., Y.-Z. Sui, Z.-Q. Yang, X.-Y. Qu, and W.-H. Zong, "A broadband dual-polarized antenna for 2G/3G/4G/5G base station applications," *Applied Computational Electromagnetics Society Journal*, Vol. 36, No. 9, 1202–1208, Sep. 2021.

[9] Kumar, S., A. S. Dixit, R. R. Malekar, H. D. Raut, and L. K. Shevada, "Fifth generation antennas: A comprehensive review of design and performance enhancement techniques," *IEEE Access*, Vol. 8, 163 568–163 593, 2020.

[10] Patel, D. H. and G. D. Makwana, "Multiband antenna for 2G/3G/4G and sub-6 GHz 5G applications using characteristic mode analysis," *Progress In Electromagnetics Research M*, Vol. 115, 107–117, 2023.

[11] Gollamudi, N. K., Y. V. Narayana, and A. M. Prasad, "A novel cow-head shaped multiple input multiple output antenna for 5G Sub: 6 GHz N77/N78 & N79 bands applications," *Progress In Electromagnetics Research C*, Vol. 122, 83–93, 2022.

[12] Tolli, A., L. Thiele, S. Suyama, G. Fodor, N. Rajatheva, E. D. Carvalho, and J. H. Sorensen, "Massive multiple-input multiple-output (MIMO) systems," *5G Mobile and Wireless Communications Technology*, Cambridge University Press, 2016.

[13] Malviya, L., R. K. Panigrahi, and M. V. Kartikeyan, "MIMO antennas with diversity and mutual coupling reduction techniques: A review," *International Journal of Microwave and Wireless Technologies*, Vol. 9, No. 8, 1763–1780, Oct. 2017.

[14] Yeo, J. and J.-I. Lee, "Design of compact broadband series-fed two dipole array antenna with top loading," in *2013 IEEE Antennas and Propagation Society International Symposium (APSURSI)*, 892–893, Orlando, Fl, Jul. 2013.

[15] Malaisamy, K., M. Santhi, S. Robinson, and S. M. Wasim, "Design and development of dipole array antenna for Wi-Fi applications," *Wireless Personal Communications*, Vol. 123, No. 4, 3375–3400, Apr. 2022.

[16] Yeo, J. and J.-I. Lee, "Size reduction of series-fed two dipole array antenna using top-loaded elements," *Microwave and Optical Technology Letters*, Vol. 55, No. 10, 2288–2293, Oct. 2013.

[17] Wasim, M. and S. Khera, "Dual band and polarised cross STDA MIMO system for the base station antenna for 5G communications," *2021 9th International Conference on Reliability, Infocom Technologies and Optimization (Trends and Future Directions) (ICRITO)*, 1–4, 2021.

[18] Haridoss, G., S. Ravimaran, J. William, M. Wasim, and M. Abdullah, "High gain series fed two dipole array antenna with reduced size for LTE application," *IETE Journal of Research*, Vol. 68, No. 2, 1084–1090, Mar. 2022.

[19] Yeo, J., J. I. Lee, and J. T. Park, "Broadband series-fed dipole pair antenna with parasitic strip pair director," *Progress In Electromagnetics Research C*, Vol. 45, 1–13, 2013.

[20] Thai, T. T., G. R. DeJean, and M. M. Tentzeris, "Design and development of a novel compact soft-surface structure for the front-to-back ratio improvement and size reduction of a microstrip yagi array antenna," *IEEE Antennas and Wireless Propagation Letters*, Vol. 7, 369–373, 2008.

[21] Chakraborty, A., B. Gupta, S. Chakraborty, and S. Dey, "Design and characterization of a Yagi Uda antenna array for weather monitoring," *2019 IEEE Radio and Antenna Days of the Indian Ocean (RADIO)*, 1–2, Sep. 2019.

[22] Yamagajo, T., Y. Koga, M. Kai, T. Tonooka, H. Sumi, and M. Hoshino, "A nobel 4G and 5G antenna solution for future smartphones," in *2018 IEEE International Symposium on Antennas and Propagation & USNC/URSI National Radio Science Meeting*, 1785–1786, Boston, Ma, Jul. 2018.

[23] Thirupathi, M. and B. Harikrishna, "Reduced mutual coupling multiband MIMO patch antenna with swastik type mushroom EBG," *Indonesian Journal of Electrical Engineering and Computer Science*, Vol. 14, No. 1, 490–494, 2019.

[24] Thakur, V., N. Jaglan, and S. D. Gupta, "Design of a dual-band 12-element MIMO antenna array for 5G mobile applications," *Progress In Electromagnetics Research Letters*, Vol. 95, 73–81, 2021.

[25] Bergmann, J. R., F. J. V. Hasselmann, L. C. P. Pereira, and M. G. C. Branco, "Reflector antenna configurations for radio base stations in cellular communications," in *1998 IEEE-APS Conference on Antennas and Propagation for Wireless Communications (Cat. No. 98EX184)*, 61–64, Waltham, Ma, Nov. 1998.

[26] Nurul, H. M. R., Z. Mansor, and M. K. A. Rahim, "Dual element MIMO planar inverted-F antenna for 5G millimeter wave application," *TELKOMNIKA (Telecommunication Computing Electronics and Control)*, Vol. 17, No. 4, 1648–1655, 2019.

[27] Douglas, T. J. and K. Sarabandi, "A high-isolation two-port planar antenna system for communication and radar applications," *IEEE Access*, Vol. 6, 9951–9959, 2018.

[28] Sehrai, D. A., J. Khan, M. Abdullah, M. Asif, M. Alibakhshikenari, B. Virdee, W. A. Shah, S. Khan, M. Ibrar, S. Jan, A. Ullah, and F. Falcone, "Design of high gain base station antenna array for mm-wave cellular communication systems," *Scientific Reports*, Vol. 13, No. 1, 4907, Mar. 2023.

[29] Hua, C., R. Li, Y. Wang, and Y. Lu, "Dual-polarized filtering antenna with printed jerusalem-cross radiator," *IEEE Access*, Vol. 6, 9000–9005, 2018.

[30] Feng, B., L. Li, J.-C. Cheng, and C.-Y.-D. Sim, "A dual-band dual-polarized stacked microstrip antenna with high-isolation and band-notch characteristics for 5G microcell communications," *IEEE Transactions on Antennas and Propagation*, Vol. 67, No. 7, 4506–4516, Jul. 2019.

[31] Gao, Y., R. Ma, Y. Wang, Q. Zhang, and C. Parini, "Stacked patch antenna with dual-polarization and low mutual coupling for massive MIMO," *IEEE Transactions on Antennas and Propagation*, Vol. 64, No. 10, 4544–4549, Oct. 2016.

[32] Wu, Q., P. Liang, and X. Chen, "A broadband $\pm 45^\circ$ dual-polarized multiple-input multiple-output antenna for 5G base stations with extra decoupling elements," *Journal of Communications and Information Networks*, Vol. 3, No. 1, 31–37, Mar. 2018.

[33] Huang, H., X. Li, and Y. Liu, "5G MIMO antenna based on vector syn1thetic mechanism," *IEEE Antennas and Wireless Propagation Letters*, Vol. 17, No. 6, 1052–1055, Jun. 2018.